A REVIEW ON BUCKLING COLLAPSES OF SIMPLE AND COMPLEX COLUMNS MADE BY PULTRUDED FRP MATERIAL

Salvatore Russo

Iuav University of Venice, Department of Design and Planning in Complex Environments, Dorsoduro 2206, 30123, Venice, Italy – russo@iuav.it

Abstract

Presented herein is a review of experimental and numerical results of the compression behavior and collapse modes of pultruded FRP (fiber reinforced polymer) columns. The aim is to propose an updated summary-review useful both in the research and in the design field. The study compares the structural performance of columns made by single pultruded shapes and complex columns, whose sections are the result of the connection of FRP pultruded profiles, of FRP-concrete and of pultruded profiles with hybrid fibers. In the specific case of the FRP-concrete column, the limitations and benefits are discussed. The survey provides some final directions on the structural behavior and on the failure modes of all the types of columns. As regards the design, the reliability of the individual models is verified and available formulas with respect to the detection of the lower value of critical load, as well as the open questions, especially for the complex columns, are presented.

Keywords: buckling collapses; failure modes; local-global buckling column; hybrid fibers; built-up columns; FRP-concrete columns;

1. Introduction

Since the early 1990s, the FRP materials commonly referred to as FRP (Fiber Reinforced Polymer) were employed in the field of civil construction. These materials have been a novelty in the engineering and architecture fields after being successfully used in naval and aviation industries due to their lightness, strength and durability. With the employment in the construction field, there was immediately a strong development in reinforcement and structural rehabilitation, while in the area of the new construction it has not been so much considered. In existing buildings, the FRP materials in the form of lamina and sheet can be glued on the surfaces of structural elements, in concrete, masonry, wood and metal materials. In most cases, FRP materials have been used to wrap columns, as shear reinforcement of masonry walls or as a flexural reinforcement of beams. Since the late 1990s, thanks to some strategic achievements [1], the possibility of using FRP materials for new construction begins to develop. From the view point of the production process, the Putrusion and Filament-Winding are most used, although other techniques are available such as Bag Molding. The level of research conducted on FRP

structures is very high and there are available technical recommendations, see ASCE 1984, DT-CNR 2007 and volumes dedicated by Agarwal et al. (1990), Eurocomp (2003) and Fiberline Manuals (2013). The state-of-the-art is particularly rich with reference to buckling, Barbero et al. (2000), Lane et al. (2002), Pecce et al. (2000); for connections [Mottram (1999)] to durability and damage [Russo (2013)] or for special applications such as sheet piles [Boscato et al. (2011)]. With regard to connections, the literature is very wide with reference to pultruded FRP frames (Bank et. al. 1994, Smith et. al. 1999, Turvey et al. 2004), particularly in presence of semi-rigid joints, (Turvey et al.1997, Cuhna et al. 2008, Minghini et al. 2009-2010), and in presence of dynamics loads (Mosallam et al. 1994). The information on the structural behavior of FRP pultruded profiles are now more than sufficient in the static field, also with reference to models and design. Some early publications on dynamic behavior of FRP structures highlight good overall performance with respect to fundamental frequency, period, and damping coefficient (Boscato et al. 2009). The remarkable lightness of the material, however, is associated with low frequencies; thereby high periods and dissipative characteristics are significantly influenced by the high deformability (Boscato et al. 2014). The structural themes related to a complex use of more pultruded profiles, for example coupled to other materials, such as concrete or steel, together with the possibility of producing built-up type or with more reinforcing fibers, need more studies (Boscato et al. 2015, Russo 2014, Boscato et al. 2014). Just what lingers research-review, entirely devoted to the analysis of structural performance and failure modes for instability of the most important element of the structural design, is the column. The survey shows some experimental and numerical results on the behavior of simple columns made by pultruded FRP material (consisting of a single shape with open or closed section) and complex columns (then coupled to another material or built-up or with more than one reinforcing fiber) in which the pultruded FRP material has a dominant role and a structural function. Some insights are devoted to aspects of design, with particular reference to the calculation of critical load and the ability to implement new prototypes of FRP columns.

2. State-of-the-art concept of column's made by FRP material

The current production of FRP pultruded profiles in structural field employable with the function of column follows in fact what is already available in the steel. It does not have a completely autonomous conceptual and still suffers the first choices excessively oriented to imitate the design principles of structural steel (Mottram 2011). The consequence is that the sections pultruded FRP resemble throughout the steel sections except for the thicknesses that in pultruded FRP are slightly higher in order to avoid local instability. For reference, one must remember that the production techniques of the elements in FRP strongly influence the design of the structural sections. This represents a limit but also an opportunity. The pultrusion, for example, as a process with predominantly longitudinal development, is more suited to the production of one-dimensional elements. Bag Moulding allows one to produce two-dimensional thin elements and the Filament-Winding is associated to the creation of structural hollow profiles. There is still yet a class of structural sections designed specifically for pultruded FRP materials. For this reason

some local interventions as the use of local stiffening elements can be adopted in construction phase. Studies on the interaction between local and global buckling which in fact is always present in the columns pultruded FRP (except for elements very slender but that cannot be actually used due to their high deformability) were consolidated in the 90s. Research suggests that the adoption of appropriate models to varying slenderness take account the compression behavior (Bank 2006), according to design by testing procedures that are particularly appropriate for this type of material. Besides, some specific works are dedicated to the failure mode of slender columns, (Barbero et al. 2000), as well as short columns (Turvey et al. 2006a). On the important role of the web-flange junction strength, some works are available in the literature (Bank et al. 1999, Turvey et al. 2006-2006 and Feo et al. 2013). It is clearly established that the shape of the cross section has a strong influence on the buckling capacity (Di Tommaso et al. 2003). The performance of the FRP open sections with wide flange are much less efficient than the sections with narrow one because of the easy onset of local instability. Even the activation of torsional buckling can influence the structural behavior of the thin open section (Timoshenko, 1961). The simultaneous presence of low values of longitudinal and transverse elastic modulus and shear modulus, together with the orthotropic material mean that the torsional and flexural-torsional instability are dominant. On the effects due to the viscosity, some studies have shown a reduction of the buckling load. On the effect of initial geometrical imperfection on buckling mode, two recent papers investigated the type and level of influence (Laudiero et al. 2014-2013). In the literature there are some initial assessments of the structural behavior of built-up FRP columns for which the formulas available for steel are however only partially reliable (Boscato et al. 2014 and Russo 2014 and Boscato et al. 2013). Particularly useful is the work cited in Keller (2002), in which the most representative realization with built-up members is investigated, even if by now many similar constructions were built. In any case, some considerations about this type of complex column may already be proposed. For example, the diffusive way of load between the various profiles making up the FRP built-up section varies considerably to changing rules for the application of the load, and deserves a further study. Similarly, formulas available today for the determination of the reduced length are not usable, and further researches on this specific subject appear useful and strategic. This type of column complex is more easily assembled with open sections with "C" or "L" shapes. It does not exclude the use of sections to "I" or "H" shape but their use appears to follow the criteria of efficiency and optimization. In any case, their use would be more appropriate in the presence of a request for a very high load-bearing capacity. For the union between the various profiles with open sections, the bolts are more reliable than glued solution. The built-up columns ensure a high increase in bending stiffness and less effect due to the shear deformability (Russo 2015). On the issue of the functioning of the connections in this type of columns, the research is still limited. However, it seems clear that the effective functioning of this type of column is strongly influenced by the proper design of the connections between the profiles. On the structural behavior of complex columns result of the union of FRP and concrete not too investigations are disposable, except some interesting works (Fam et al. 2005-2005 and 2003). This type of column is realized with hollow pultruded FRP shapes (square, circular or rectangular section) which will also function as formwork with respect to concrete which will be included in. From a viewpoint

of potential performances, it is expected that the concrete delays the onset of the local buckling phenomena allowing its use for higher values of slenderness. An increase of the bearing capacity is expected when compared to the use of only one section in FRP, without which the integration with the concrete would have no effect. The influence of the mode of application of the load (if applied to the entire section or to the only part in concrete) was treated in some research; as well as the assessment of the effects of wrapping of hollow FRP profile than the concrete (Boscato et al. 2006). For hybrid pultruded FRP sections (with reinforcing fibers of various kinds such as glass and carbon) computational methods that provide for the homogenization of the mechanical characteristics of the different fibers have to be used (Agarwal et al. 1990) in order to determine the mechanical parameters more correctly for the calculation of the buckling loads. Some experimental investigations show that the performance of hybrid all-FRP profiles are still unreliable. Some general observations may arise on the structural design of the columns characterized by the use of hyperlight pultruded FRP material. Good performance are expected also in all FRP frame at ultimate limit state (Casalegno et al. 2015). Figure 1 refers to an all FRP construction, (Russo et al. 2012, Boscato et al. 2012) and allow some specific reflections. It is the use of built-up pultruded FRP columns made by bolted connections of four "C" shape inserted into reinforced concrete plinths with function of foundation surface. In this case, the design was influenced by aspects of emergency and very specific needs. For example, the need for a roof structure and a floor support which is not too unwieldy flooring historical and, consequently, the need to anchor the light structure to the ground with additional masses. The same figures confirm, however, as the design with FRP pultruded profiles still too follows the design principles of steel. This is evidenced in particular by the excessive size of the sections of the pillars and cross bracing struts, (see Figure 1). While these choices appear understandable and reasonable, but too conditioned by excesses of structural safety, on the other hand it is now necessary to calibrate more specifically in the design of FRP on the basis of the characteristics of the material, even in the face of a level of knowledge now mature. The detail of Figure 1 confirms the easy process of the pultruded FRP material in combination with other materials. The same figure, on the other hand, relative to a construction already erected in 2009, highlights the absence of any effects caused by the concrete than the FRP material. A further improvement of the mechanical interaction between the two materials can be obtained in any case interposing epoxy resin.

3. Experimental results

In summary form are reported the most significant experimental results obtained. For all columns are presented, with the same sequence, the pictures of the setup and testing of the collapses, the table with the overall results of the geometrical and mechanical characteristics of the columns, and the most significant load-displacement curves. The average values of the characteristics of the pultruded FRP profiles declared by the manufacturer and used for the tests are shown in Table 1 (Topglass Manual, 1963).

3.1 Simple Column - single element

The columns subjected to compression test have "I", "H" and "C" shapes. For each test the experimental load-displacement curves with lateral displacement detected on time with transducers, and the images of the collapses are showed. Figure 2 and Figure 3 shown the results for "I" shape 120 x 60 x 8 mm; Figure 4 and Figure 5 refer to the result on "H" shape 200 x 200 x 15 x 10 mm. Overall, the results shown by Figure 2 to Figure 5 highlight, regardless of the geometry of the section, the presence of a local buckling inversely proportional to the slenderness and a global buckling directly proportional to it. The photographic surveys of the stages of collapse illustrate the lack of interaction between local and global buckling in the profile with the higher value of slenderness, (Figure 3), while it is present in all other profiles. The profiles more stubby collapse instead in consequence of the interaction between local buckling and crushing, as confirmed by Figure 2. The summary of the final values of the maximum load indicated in Tables 2 and 3 respectively for the columns with "I" and "H" shape show the performance of the overall structural performance, while the load-displacement curves confirm the elastic-brittle behavior.

3.2 Complex Column – FRP/Concrete case

The realization of columns result of the union of FRP pultruded profiles and concrete is particularly suitable in the presence of hollow shapes, so that the concrete there can be inserted in the fluid state, and these shapes can also perform the function of the formwork. The experimental investigation shows the case of GFRP/Concrete columns having square and circular section for distinct values of slenderness. The survey was preceded by tests performed on only pultruded FRP profiles, in order to make more complete the analysis for comparison. The results relating only to all FRP profiles are shown in Table 4. The collapse most significant relating to stubby columns is shown in Figure 6. The summary of the values of the maximum load for FRP/Concrete columns is shown in Table 5. Test results show a strong influence of the FRP shape on structural performance. The analysis of the experimental results shows that the increased vulnerability of the geometric square section caused by the presence of the angles - with respect to the circular one which ensures a more appropriate effect of wrapping - is attenuated by the size of the thickness. In the case of the FRP square hollow shape it is in fact twice than the circular shape and final load values resulting appreciably affected. The comparison between the performance of the FRP hollow profiles and the same sections filled with concrete in the case in which with the load is applied both to the entire cross section and only to the concrete, is indicated in the diagrams of Figures 7. It is interesting to note that the benefit provided by the use of concrete coupled to pultruded FRP profiles is more important in the circular shape than the square one. This is due primarily to its form, the most suitable to ensure an effective wrapping effect, especially when the load is applied only to the concrete, and to the reduced thickness, which favors a better optimization of the use of the two coupled

materials. Figure 7 shows in particular that the circular profile of FRP has much lower performance compared to the case in which it is filled with concrete. For high value of thickness and square shape said beneficial effect is reduced, and even the only square profile FRP shows a greater stiffness than with concrete. This can be also depended upon the fact that especially for high loads the concrete has favored the triggering of local buckling in the FRP shape anticipating the collapse. For FRP/Concrete columns with values of slenderness substantially higher, the most significant failure modes of the slender column is shown in Figure 8. The curves crushing load of some FRP/Concrete columns tested are indicated in the diagram of Figure 9, with the lateral displacements detected. It is known as the failure modes remain of elastic-brittle, since the concrete stiffens further the complex column with respect to only the FRP shape. Conversely, the more important lateral displacements that appear close to the collapses are achieved when the column is made by only FRP shape.

3.3 Complex Column - Built-up case

The complex built-up columns are an assemblage of FRP pultruded profiles with "C" shape, connected with steel bolts. The columns analyzed belong to two types of cross sections (Boscato et al. 2015). On type of section is constituted by smaller "C" shape and has four bolted connections point along its length; the other type is constituted by larger "C" shape and has a total of five bolted connections point along its development, as shown in detail. The tests were performed on both types of columns by first applying the load to the two central "C" shape that make the web, then applying the load to the entire built-up section. The boundary conditions were designed by inserting a sphere between two plates, one inside one outside, in order to allow any type of displacement during the increasing of the load or any torsional phenomena. The failure modes for columns subjected to the load applied only to the web are shown in Figure 10. In particular, the phenomena of crushing at the ends and the local buckling occurred in areas further away from the bolted connections lines, are captured. The crisis mechanism relative to the columns in which the load is applied to the entire section is significantly difference with local buckling and a significant global torsional buckling. The difference in terms of load-bearing capacity is evident from the analysis of Figure 11, in which the maximum loads achieved in the case of load applied to the entire cross section are four times higher than those obtained when the column is loaded only through the web. In this latter case the column does not behave like a real built-up column, but as a column formed by only two FRP profiles and then reinforced with other two external "C" shape connected to it with bolts. The considerable difference in behavior does not affect the initial stiffness, which in fact remains the same, but the values of maximum load. In the event that all four "C" shapes are contemporary stressed, even connections bear an important shearing actions, for the benefit of the final performance.

3.4 Complex Column - hybrid fibers case

The diagram of Figure 12 refers to "I" pultruded shape with glass fibers, arranged in the web, and with carbon fibers arranged in the flanges together with other glass fibers according to the percentages by volume indicated in Table 1. For the position of the carbon fiber inside the section see photographic detail inside the diagram of Figure 12. The hybrid pultruded profiles tested in compression and compared to profiles reinforced with a single fiber show a similar mode of collapse but with a post peak less rigid and maximum load values significantly reduced. The diagram of Figure 13 shows the comparison between two "I" shapes having the same cross section and height, but different type of fibers. The profiles with the single fiber glass exhibits higher values of maximum load compared to the hybrid profile (glass + carbon). It is noted that the curves of the mono-fiber profiles are fully elastic-brittle while those with two types of fiber show increased deformability in the phase of softening.

4. Models and Design's aspects

Following an overview related to the models and closed formulas already available for simple and complex all-FRP columns tested. The overview includes also proposals about the cases in which the reliable analytical approaches are not yet available. In the case of simple columns, the literature and the related technical recommendations appear very solid. While for all the complex pultruded FRP columns investigated by experimental test – especially the FRP/Concrete and hybrid ones - the analytical methods still need new approaches than the already existing formulas.

4.1 Simply columns – single shape case

The models and the closed formulas are by now reliable and efficient for simple column made by pultruded FRP hollow profiles or open cross section. A first distinction, even if not perfectly including, could be proposed between open sections with two axis of symmetry in which the local instability play an important role, and sections with only one axis of symmetry, subjected also to torsion instability. For both cases, the introduction of the availability formulas can be first assumed in function of the slenderness value. For the higher values, the following formula are consolidated and can be applied:

$$P_{cr(e)} = \frac{\pi^2 \cdot E \cdot J_{\min}}{(L_0)^2} \tag{1}$$

$$P_{cr(G)} = \frac{P_{cr(e)}}{1 + \frac{\chi \cdot P_{cr(e)}}{A_{shear} \cdot G}} \tag{2}$$

The well known (1) is widely employed when the expected flexural buckling is relevant and dominant (Timoshenko 1961), while the (2) considers the influence of the shear deformability that in FRP material is sensitive than the steel (Engesser 1889). In both formula E represents the modulus of elasticity in compression, J_{min} the lower moment of inertia, L_0 is the free length (or reduced length) in function of the boundary conditions, χ is the shear factor, A_{shear} is the shear resistant area and G is the shear modulus. The utility of (2) is putting into account the shear deformability with results more appropriated than formulation (1). For intermediate values of λ intervenes local buckling which reduces the value of the global one. For the calculation of the local critical load have been proposed various formulas extracted directly from previous experiences with the steel. Those following proposals, which take into account the bending stiffness of orthotropic plates appear more solid and reliable (Barbero et al. 2000, Kollar 2003). In the case of open section, the local critical load in the local flanges can therefore be calculated with the following relationship:

$$F_{loc(f)} = \frac{\pi^2}{L^2_w} \cdot \left[3.125 \cdot \sqrt{D_{11} \cdot D_{22}} + 2.33 \cdot \left(D_{12} + 2 \cdot D_{66}\right)\right] \quad (3)$$

where with the term $F_{loc(f)}$ can be intended the local buckling load in the flange of the "I, "H" or "C" shapes. Besides with the general symbol D we utilize the flexural stiffness of orthotropic plates that in detail are D_{11} equal to (E_c x t^3)/12 x (1-ν_{lt} x ν_{lt}), D_{22} equal to (E_{tl} x t^3)/12 x (1-ν_{lt} x ν_{lt}), D_{66} is equal to (G x t^3)/12 , D_{12} is equal to ν_{lt} x D_{22}; ν_{lt} and ν_{tl} are the Poisson's coefficients in longitudinal and transversal direction; L_w is the width of each plate analyzed. For the calculation of the value of local buckling for the web, will be applied the following relation in according with the previous (3) and as written by Kollar (2003):

$$F_{loc(w)} = \frac{\pi^2}{L^2_w} \cdot \left[4.53 \cdot \sqrt{D_{11} \cdot D_{22}} + 2.62 \cdot \left(D_{12} + 2 \cdot D_{66}\right)\right] \quad (4)$$

For the evaluation of the interaction between local and global instability a partly empirical procedure, but now widely established, can be used, as indicated by Bank (2006). The critical load that takes into account the interaction is defined in the following way:

$$P_{cr} = K_{g/l} \cdot P_{loc} \quad (5)$$

In which P_{loc} is the load that triggers the local buckling of reference when the columns are stubby, $K_{g/l}$ is a coefficient that takes into account the interaction between global and local buckling given by the following formula:

$$K_{g/l} = K_\lambda - \sqrt{K_\lambda^2 - \frac{1}{c \cdot \lambda^2}} \quad (6)$$

with K_λ equal to:

$$K_{\lambda} = \frac{1+\left(\frac{1}{\lambda^2}\right)}{2 \cdot c} \tag{7}$$

In (6) and (7) the term c is an empirical constant whose value in the literature is assumed variable between 0.65 and 0.80 as a function of a more or less conservative approach. The value of λ coincides with the following relation:

$$\lambda = \frac{K \cdot L}{\pi} \cdot \sqrt{\frac{P_{loc}}{EJ_{\min}}} = \sqrt{\frac{P_{loc}}{P_e}} \tag{8}$$

where EJ_{min} is the value of the bending stiffness corresponding to the minor axis of the section. The trend of the value of $K_{g/l}$ (equal to χ) referred to the preceding (6) is indicated in the well known diagram of Figure 14 as a function of the value of dimensionless λ referred to (8) and Bank (2006). Beside an useful work related to the use of the curve indicated in Figure 14 is available in Vanevenhoven (2010). The critical height of the column at which will start the interaction between local and global instability may be determined using the (1) or (2); the value of L_0 in function of P_{loc} using the (1) will be equal to:

$$L_0 = \sqrt{\frac{\pi^2 E \cdot J_{\min}}{P_{loc}}} \tag{9}$$

whose terms are already known.

4.2 Complex columns – FRP/Concrete case

Nor consolidated models or numerical approaches are still available to understand the buckling in presence of FRP/Concrete columns. One possibility way seems to be relate to the use of models already applied for the steel-concrete columns, as that indicated in the correspondent Eurocode (1994), with some corrections. By the way, two different type of formulations available for steel-concrete cross sections could be employed with some modification. In the first approach, the well-known Euler's formula, with the stiffness flexural modified value has been utilized (Shneider 1998). To determine the ultimate strength values P_{cr1}, we use the formula (1), where in the presence of FRP/Concrete columns the elastic stiffness flexural EJ_{min} becomes:

$$(E \cdot J)_1 = E_{FRP} + J_{FRP} + S_c \tag{10}$$

In the (10) all symbols have an evident meaning except the S_c that is the stiffness of the concrete core given by the following:

$$S_c = 0.83 \cdot E_{Ces} \cdot J_C \tag{11}$$

where the coefficient 0.83 is the multiplier to transform the cylindrical concrete test in the cubic one and E_{Ces} is the modulus of elasticity of concrete assumed equal to the following:

$$E_{Ces} = \frac{E_{\sec}}{\gamma_c} \tag{12}$$

With E_{sec} equal to the secant modulus of elasticity of concrete in compression and γ_c is a safety coefficient for stiffness. Generally the approach proposed through (1) and the modifications showed from (10) to (12) is very similar to the approach of the Eulerian buckling and the presence of two different materials is accounted inside the new combined definition of the flexural stiffness as showed in (10). Another approach that is particularly calibrated for circular FRP/Concrete even if starting initially from steel-concrete cross section, foresees the calculation of the ultimate strength as following:

$$P_{cr2} = A_{FRP} \cdot F_{cr} \tag{13}$$

with A_{FRP} equal to the area of the FRP section and F_{cr} assumed as the following two formulations, both in function of the slenderness parameter $\lambda_2{}^2$; so we obtain:

$$F_{cr} = \left(0.658^{\lambda_2^2}\right) \cdot F_{mus} \qquad \text{for } \lambda_2<1.5 \tag{14}$$

$$F_{cr} = \left(\frac{0.877}{\lambda_2^2}\right) \cdot F_{mus} \qquad \text{for } \lambda_2>1.5 \tag{15}$$

In both previous formulations the value of $\lambda_2{}^2$ is defined as:

$$\lambda_2^2 = \left(\frac{L_0}{\rho_{FRP} \cdot \pi}\right) \cdot \left(\frac{F_{mus}}{E_m}\right) \tag{16}$$

in which ρ_{FRP} is the radius of gyration of inertia assumed as following:

$$\rho_{FRP} = \sqrt{\frac{J_{FRP}}{A_{FRP}}} \tag{17}$$

and F_{mus} and E_m are respectively the modified values of ultimate value of strength and modulus of elasticity for the FRP/Concrete columns, so defined:

$$F_{mus} = F_{FRP(E)} + 0.85 \cdot f_c \cdot \left(\frac{A_c}{A_{FRP}}\right) \tag{18}$$

$$E_{mus} = E_{FRP(E)} + 0.40 \cdot E_c \cdot \left(\frac{A_c}{A_{FRP}} \right) \quad (19)$$

To determine the above values we assume that $F_{FRP(E)} = P_{cr(FRP)}/A_{FRP}$, and that $P_{cr(FRP)}$ is equal to:

$$P_{cr(FRP)} = \frac{F}{1 + \frac{F}{P_{el}}} \quad (20)$$

with $F = A_{FRP} \; x \; f_{FRP}$ with f_{FRP} equal to compressive strength of FRP profiles and $P_{el} = \pi^2 \text{ x } (E_{FRP} \text{ x } J_{FRP})/L_0^2$. The two models proposed for complex columns FRP/Concrete aim to describe the performance through a detailed definition of the flexural stiffness which takes better account of the two materials. The calculation model of P_{cr2} is, however, more interesting as it does depends on more parameters as well as the percentage of FRP compared to the steel one, the Eulerian critical load value previously determined for the FRP profile and the slenderness**.**

4.3 Complex columns – built-up case

The models and the formulas available are only partially reliable for all FRP built-up columns since that they are referred to steel for which the way of connection between the profiles that made the composed cross section is often generated by welded action that cannot be used in presence of pultruded FRP material. Nevertheless, the base of some of the available formulas appears still usable at the outset to understand the order of magnitude of the maximum load expected. This is the case, for example, of the following formula (Timoshenko 1961):

$$P_{cr(b-u)} = K_{cr} \cdot \frac{1}{1 + K_{cr} \cdot \left(\frac{a \cdot b}{12EJ_{tr}} + \frac{a^2}{24EJ_{iL}} + \frac{\chi \cdot a}{b \cdot A_{tr} G} \right)} \quad (21)$$

where the flexural stiffness EI_{tr} is usually considered in presence of battens and here involves the channels that constitute the web of the built-up column; EI_{iL} is the flexural stiffness of one singular channel, A_{tr} is the cross-section of the two channels just mentioned; while a is assumed equal to the longitudinal distance between the intermediate bolted connections and b equal to the transversal distance between the center of the masses of the more distant profiles. Both the flexural stiffness and a and b values refer, as mentioned, to a built-up welded steel column but these values may still be reformulated for the built-up sections here analyzed. In addition K_{cr} is the value of Eulerian critical load calculated by means of (1).The formula (22) for calculation of the reduced length appears very limited in terms of use in the presence of FRP material. Recent applications have shown not compatible values (Boscato et al. 2015, Russo 2014, Boscato et al. 2014). In detail the found values show the need for a sensitive recalibration of the (22) to become more able to consider the actual deflection and deformation of FRP built-up columns.

$$l_r = l \cdot \sqrt{1 + \frac{\pi^2 EJ_{(b-u)}}{l^2} \cdot \left(\frac{a \cdot b}{12 EJ_{h-c}} + \frac{a^2}{24 EJ_{v-c}} + \frac{\chi \cdot a}{b \cdot A_h \cdot G} \right)} \quad (22)$$

In the presence of a simplified calculation to evaluate the critical load, appears still not clear the choice of the slenderness more appropriate to use. For built-up columns are available some formulations (Turvey et al. 2006, Manual Steel 2006). In particular in the (23), where A_1 is the cross-section of the single channel and is N_{1cr} its critical load, as following:

$$\lambda_{eq} = \sqrt{\frac{2 \cdot E \cdot A_1}{N_{1cr}}} \quad (23)$$

The formulas (24) and (25) in a more targeted way take into account the interaction between global slenderness of the column and slenderness of the most vulnerable element among the local connections. The symbols λ_{gl}, and λ_o respectively coincide with the slenderness of the built-up column as a whole, and the slenderness of the single channel, as indicated here:

$$\lambda_{eq} = \sqrt{\lambda_{gl}^{\ 2} + \pi^2 \frac{EA}{GA_{shear}}} \quad (24)$$

$$\lambda_{eq} = \sqrt{\lambda_1^{\ 2} + \lambda_o^2} \quad (25)$$

Formulas (24) and (25) that take into account both the slenderness connected to the stiffness offered by the entire section and the flexural stiffness of the more slender element, appear more appropriated.

4.4 Complex columns – hybrid FRP fibers case

For this type of columns, there are neither models nor formulations available. It seems reasonable to use a formula already used for simple columns to determine local and global instability. The presence of two reinforcing fibers together with the matrix used in the pultrusion process requires however an in-depth analysis. In this sense, the Rule of Mixtures (Agarwal et al. 1990) can provide adequate support to take account of all the reinforcing fibers present and calculate the real mechanical parameters. The Rule of Mixtures offers the following formulation:

$$\upsilon_{frp} = \upsilon_f + \upsilon_m \quad (26)$$

having indicated with υ_{frp} the volume of the composite material, with υ_f the volume occupied inside from the fiber and with υ_m the volume occupied by the matrix. In the case of structural elements pultruded with the double fiber, the (26) may be rewritten as:

$$\upsilon_{Hfrp} = \upsilon_{Gf} + \upsilon_{Cf} + \upsilon_m \quad (27)$$

with the following percentages for the three components:

$$V_{Gf} = \frac{\upsilon_{Hfrp}}{\upsilon_{Gf}} \qquad V_{Cf} = \frac{\upsilon_{Hfrp}}{\upsilon_{Cf}} \qquad V_m = \frac{\upsilon_{Hfrp}}{\upsilon_m} \tag{28}$$

where υ_{Hfrp} represents the volume of the hybrid FRP material and υ_{Gf} , υ_{Cf} respectively the percentage by volume of the reinforcing fiber made by glass and carbon. Considering the case of the investigated hybrids profiles – Figures 12 and 13 – the equilibrium in the same direction of the applied load allows to write:

$$P_{Hfrp} = P_{Gf} + P_{Cf} + P_m \tag{29}$$

$$P_{Hfrp} = \sigma_{Hfrp} \cdot A_{Hfrp} = \sigma_{Gf} \cdot A_{Gf} + \sigma_{Cf} \cdot A_{Cf} + \sigma_m \cdot A_m \tag{30}$$

Assumed now, as it is, that in presence of the pultrusion process technology the fibres are parallel and then that the percentage in volume indicated in (28) coincides with the percentage of the correspondent areas - or fractions of areas - the following relation can be proposed:

$$V_{Gf} = \frac{A_{Gf}}{A_{Hfrp}} \qquad V_{Cf} = \frac{A_{Cf}}{A_{Hfrp}} \qquad V_m = \frac{A_m}{A_{Hfrp}} \tag{31}$$

that allows to write the (30) as the next:

$$\sigma_{Hfrp} = \sigma_{Gf} \cdot V_{Gf} + \sigma_{_{Cf}} \cdot V_{Cf} + \sigma_m \cdot V_m \tag{32}$$

that is the consequent of the assumption of the validity of the Hooke's Law and of the correspondent linear stress-strain relation. The (32) will be rewritten as following

$$E_{Hfrp} = E_{Gf} \cdot V_{Gf} + E_{Cf} \cdot V_{Cf} + E_m \cdot V_m \tag{33}$$

Finally, the determined value of E_{Hfrp} will be therefore employed in flexural stiffness to determine through (1) or (2) the critical load values.

5. Discussion of the results and open questions

Following the first reflections on the comparison between experimental and numerical results with particular reference to complex columns for which some themes are still open and the need to recalibrate the available formulations is significant. The first part of the discussion is devoted to an experimental evaluation about the failure modes of the columns investigated. The second part presents an analysis of the reliability of the proposed models and formulas through comparison with experimental results.

5.1 Experimental

With reference to the simple columns, the modes of collapse detected consolidate what is already known on the buckling of pultruded FRP columns. The modes of failure are always conditioned by the local buckling that in function of the slenderness influence more or less the global buckling. The orthotropic material, the high deformability and the shape are the factors that most influence the modes of failure. As regards the behavior of the complex FRP/Concrete columns more slender and with square shape, the collapse happens to very high loads and is manifested by the vertical lines of fracture in coincidence of the edges; this may have several explanations. On the one hand it confirms the presence of vulnerability at the corners of FRP shapes as consequence of the pultrusion process. The type of crisis was also influenced by the lateral thrust of the concrete contained therein. Equal FRP shape without concrete is instead characterized by a collapse due by the interaction between crushing at the ends and overall flexural buckling. As regards the mode of crisis in the circular FRP/Concrete column, loads achieved are lower than the square ones, this is due to higher slenderness and to the much smaller thickness profile. The red line (Figure 8) helps to grasp the phenomenon of global flexural instability in absence of local crises. The excellent performance of the FRP/Concrete columns when the section is circular and the thickness reduced is confirmed; the wrapping effect is effective and benefits are high. For the built-up columns the mode of charge is undoubtedly the variable of greater weight. The involvement or not of all cross section available strongly affect the structural behavior of the entire system. It thus passes from a column with a real built-up behavior (when the entire cross section is subjected to compression) to a kind of reinforced column when the load is applied to only two of the four profiles. Two types of built-up column analyzed appears however still limiting with respect to trying to obtain observations conclusiveness and generalizable. The values of P_{cr} obtained are further confirmation of the fact that the two modes of charge determine as many structural running significantly different. When the load is applied to the entire cross section, the maximum loads in fact achieved very high values compared to the case where the load is applied only to the web. This shows that column type BC2 behaves like a built-up one, while column BC1 of Figure 10 behaves as a column composed by two profiles and then reinforced by other two profiles that then have only the function of delaying the onset of global flexural instability. The differences caused by the distinct mode of application of the load involve also the functioning of the connections. In the case BC2 bolts are useful to the running of the column as a real built-up column and work both under shear and bearing stresses; in the case BC1 they work only to friction. Hybrid columns performance gave results very less homogeneous with respect to identical columns pultruded with a single fiber. The presence of two types of fibers appears to have reduced the mechanical homogeneity of the profile anticipating the brittle collapse processes and local failure. To date, the use of pultruded FRP profiles with two fibers does not appear to be sufficiently reliable.

5.2 Model and design aspects

As is now ascertained, Euler's formula (1) is applicable only in the presence of high values of λ, vice versa is not realistically be used given the high deformability of pultruded FRP material. In the presence of intermediate values of slenderness, said formula (nor (2) that takes into account the shear deformation) could reasonably be used. This is confirmed by comparison of the diagram of Figure 15 for different values of λ. The formulas (3) and (4) appear the most appropriate for the determination of the local critical load that often is the lowest and is then used in structural design. The formulas (5) to (8) are now well established for the evaluation of the interaction between local and global buckling. In the latter case, the use of an experimental comparison is appropriate and the use of the coefficient *c* appears to be reliable. A first tentative of comparison between the experimental results obtained for simple columns and the above mentioned formulas through which is possible to draw Figure 14 has been attempted; nevertheless, the too high difference in term of λ values, as confirmed by the comparison with Figure 15, prevented this. The expectation is in any case that the experimental results should confirm the trend of the bolted curve (Figure 14) and the variation of the χ value. Diagram of Figure 15, however, confirm the utility of the diagram of Figure 14 about the evaluation of the interaction between local and global modes of buckling in simple columns. Complex FRP/Concrete columns are particularly influenced by the geometry of the FRP profile and by the wrapping effect that it plays. The FRP profiles with square section appear more vulnerable than the circular one. Table 6 shows the comparison between the experimental results obtained in Section 3.2 and the results obtained with the models proposed for the determination of P_{cr1} and P_{cr2}. Table 6 also shows how the assessment of P_{cr1} is less refined than the formulation that provides P_{cr2}. With regard to the FRP built-up complex columns, Table 7 summarizes the comparison between experimental and numerical data calculated with the equations (1), (2) and (21). Table 7 in particular refers to the values of the critical load and its variation in function of slenderness considered according to the formulas (23), (24) and (25). Table 7 shows also in detail the difference between the values of reduced length calculated with the formula (22) and the values of the actual distances between the connections and the height of the column. Table 8 refers to some results already obtained (Boscato et al. 2015) , about a comparison between two FEM models (first developed the eigenvalue approach and then a second based of geometrical non linearity) and the experimental values. The models capture adequately the behavior of the columns in the case where the load is applied only on two of the four "C" shape that constitute the section; while are inadequate when the load is applied to the entire built-up cross section. As regards the hybrid columns, the application of equation (34) for the calculation of the modulus of elasticity and the next using of the formula (2) have provided the values of the global critical load indicated in Table 8, compared with the experimental results. The numerical values found are always higher than the experimental values. This appears to confirm the tendency already detected from experimental side (Figure 13), for which the placing of a higher value of the fiber's modulus of elasticity does not guarantee with respect to a consequential increase in the overall structural performance. It should also be noted that in the face of the need to refine the technique of pultrusion where there are multiple fibers, the use of pultruded profiles hybrids seems more appropriate in presence of element subjected to tension or flexural stresses as cables or beams.

6. Conclusions

On the basis of the review-research related to the failure modes of pultruded FRP simple and complex columns, the following conclusions can be proposed.

From the experimental viewpoint:

- the investigations of simple and complex pultruded FRP columns have shown that the interaction between local and global buckling is influenced by the material mechanical properties, the λ value and the entity of initial imperfections when they are not negligible. Neglect the importance of the local-global buckling interaction could give important mistakes in design;

- the performances of the majority tested columns appear very high particularly in relation to the maximum loads reached. This evaluation is valid unless the hybrid columns, whose behaviour appears still uncertain and less reliable probably due to the need to improve the pultrusion process in presence of more than one type of fibre;

- the FRP/concrete complex columns result very efficient and generally easy to create with great potential for real applications. The shape of the pultruded FRP profiles strongly influence the failure mode. The hollow circular one is more performant as wrapping effect than the square cross section and - more generally - than sections with straight lines and corners. The local buckling remains dominant even if exalted or reduced by the concrete in relation to the ratio between the maximum dimension of the FRP profile and its thickness;

- the all FRP bolted built-up columns appear strategic from the conceptual point of view and outline a challenge due to the very high level of maximum load reached. Their employment deserve attention and could be very common. The interaction between different buckling and related failure modes is important and influential as expected by the number and type of connection along each column. In detail, the role of bolted connections, even if less investigated in the review mainly dedicated to the global failure analysis, gave difference in the performance increase.

From the model and design viewpoints:

- for simple columns made by one pultruded FRP profile, the models showed appear solid and widely employed. The need to take into account the local buckling as dominant characteristics of the collapse mode is a strongly held requirement. In design, the preliminary comparison between the all potential buckling's values (so through the comparison of formulas (2) with (3-4) and also with (5)) - must be done every time as a fixed procedure to obtain the lower value of the critical load that will be used for the final design and calculation of the column;

- in detail for simple columns made by one pultruded FRP profile, the evaluation of the entity of the interaction between local and global buckling have to be always considered through formulas from (5) to (9);

- for pultruded FRP built-up columns the way of mode of charge (on the entire cross section or only to the flanges) and the consequent diffusive phenomenon is the first point to understand and decide the better model that can be used. A first reliable calculation could be done through the appropriate slenderness (as presented in the formulas (24) and (25)) and then applying the (1) or (2). Nevertheless, this kind of calculation will result in any case still too conservative and the application of the (21) is suggested. The definition of the more correct formulation to obtain the reduced length is still an open question that needs dedicated research. The (22) is not yet applicable and the calculation of the reduced length as if the column is not built-up but simple one with the equivalent flexural stiffness and in function of the boundary conditions, is suggested;

- for the FRP/concrete complex columns, the model proposed by (13) to (20) appeared reliable and derived by the Eurocode approach for steel-concrete composed cross sections. This method resulted efficient and not too conservative as showed by the comparison with experimental results. A preliminary analysis regarding the geometrical compatibility between the FRP and concrete materials is suggested to better design the wrapping effect of the hollow FRP shape. This means the only real benefit in term of structural concept and performance of this kind of column;

- for hybrid FRP complex columns the application of the Rule of Mixtures, (33), resulted well used to determine the most dominant mechanical parameter as the modulus of elasticity; then the use of (2) to obtain the critical load will be reliable.

Aknowledgments

The author particularly thanks to TopGlass (Italy) to supply all the FRP pultruded material to realize the research. Thanks also to Ph.D.Giosue' Boscato for his support.

7. References

Agarwal BD, Broutman LJ.,1990. Analysis and performance of fiber composites, Second Edition. Whiley InterScience

ASCE, 1984. "Structural plastic design manual", American Society Civil Engineering, Vol.1

Bank LC, Mosallam AD and McCoy GT., 1994. Design and performance of connections for pultruded frame structures. J. Reinf. Plast. Comp.; 13(3): 199-212.

Bank, L. C., 2006. *Composites for Construction - Structural Design with FRP Materials*, John Wiley & Sons, N.J.

Bank LC, Yin J, 1999. Failure of web-flange junction in post buckled pultruded I-beams. J. Compos. Constr., 3(4), 177-184.

Barbero, E. J., Dede, E. K., Jones, S., 2000. "Experimental Verification of Buckling-mode Interaction in Intermediate-length Composite Columns", *International Journal of Solids and Structures*, 37(29), 3919-3934.

Barbero EJ, Turk M., 2000. Experimental investigation of beam-column behaviour of pultruded structural shapes. J. Reinf. Plast. Compos., 19(3), 249-265.

Boscato, G., Mottram, J., Russo, S., 2011. "Dynamic Response of a Sheet Pile of Fiber-Reinforced Polymer for Waterfront Barriers", *Journal of Composite for Construction*, ASCE, 15(6), 974–984.

Boscato, G. and Russo, S., 2009. "Free Vibrations of Pultruded FRP Elements: Mechanical Characterization, Analysis, and Applications", *Journal of Composite for Construction*, ASCE, 13(6), 565-574.

Boscato G, Russo S., 2014. Dissipative capacity on FRP spatial pultruded structure. Composite Structures; doi: http://dx.doi.org/10.1016/j.compstruct.2014.03.036

Boscato G., Casalegno C., Russo, S., 2015. Performance of built-up columns made by pultruded FRP material, Composite Structures Journal, Elsevier, 121, 46-63, http://dx.doi.org/10.1016/j.compstruct.2014.11.022

Boscato G, Casalegno C, Mottram JT, Russo S., 2014. Buckling of Built-Up Columns of Pultruded Fiber-Reinforced Polymer C-Sections. J. Compos. Constr.; 18(4) 0.1061/(ASCE)CC.1943-5614.0000453.

Boscato G., Casalegno C. Mottram JT, Russo S., 2013. "Buckling of GFRP pultruded built-up columns", Advanced Composite in Construction, ACIC 2013, Conference Proceedings, pp. 178-189.

Boscato G., Russo S., 2006. "Concrete-Filled GFRO Hollow Profiles Subjected to axial load", Second *fib* Congress, June 5-8, Naples, Italy.

Casalegno C., Russo, S., 2015. Pushover analysis of GFRP pultruded frames, Mechanics of Composite Materials, Vol.51, No.5, November.

Cunha J., Foltête E and Bouhaddi N., 2008. Evaluation of stiffness of semi-rigid joints in pultruded profiles from dynamic and static data by using model updating technique. Engineering Structural; 30(4): 1024-1036.

Di Tommaso, A. and Russo, S., 2003. "Shape Influence in Buckling of GFRP Pultruded Columns", *Mechanics of Composite Materials*, 39(4), 329-340.

Engesser, F., 1889. "Ueber die Knickfestigkeit gerader Stabe", *Zeitschrift für Architekter und Ingenieurwsen*, 35(4), 455-462 (in German).

Eurocode 4, 1994. Design of Composite steel and concrete structures – Part 1-1: general rules for Buildings, February 1995, UNI ENV 1994 1-1

Fam, A., Schnerch, D. and Rizkalla, S., 2005. "Rectangular Filament-Wound GFRP Tubes Filled with Concrete under Flexural and Axial Loading: Experimental Investigation", ASCE Journal of Composites for Construction, January/February. Vol. 9, Issue 1, pp. 25-33.

Fam, A., Mandal, S. and Rizkalla, S., 2005. "Rectangular Filament-Wound GFRP Tubes Filled with Concrete under Flexural and Axial Loading: Analytical Modeling", Journal of Composites for Construction, January/February. Vol. 9, Issue 1, pp. 34-43.

Fam, A., Greene, R. and Rizkalla, S., 2003. "Field Applications of Concrete-Filled FRP Tubes for Marine Piles", ACI Special Publications, November. SP-215, pp. 161-180.

Feo L, Mosallam AS, Penna R., 2013. Mechanical behaviour of web-flange junctions of thin-walled pultruded I-profiles: an experimental and numerical evaluation. Compos Part B-Eng; 48:18-39.

Fiberline, 2013. Design manual for structural profiles in composite materials. *Fiberline Composites A/S*, Kolding, Denmark.

Guide for the Design and Construction of Structures made of FRP pultruded Elements, national research Council of Italy, 2008. DT CNR 2007, Rome, October

Handbook, 2010.The international Handbook of FRP Composites in Civil Engineering, Taylor & Francis LLCC

Keller T., 2002. Fibre reinforced polymers in building construction, Proceedings of International Association for Bridge and Structural Engineering Symposium, towards a better built environment, Melbourne.

Kollar, L. P., 2003. "Local Buckling of Fibre Reinforced Plastic Composite Structural members with Open and Closed Cross Section. Journal of structural Engineering, ASCE.129:1503-1513

Lane, A. and Mottram, J.T., 2002. "The Influence of Modal Coupling upon the Buckling of Concentrically Pultruded Fibre-reinforced Plastic Columns", *Proceedings of the Institution of Mechanical Engineers Part L: J. Materials - Design and Applications*, 216 133-144.

Laudiero F, Minghini F, Tullini N., 2014. Buckling and post buckling finite element analysis of pultruded FRP profiles under pure compression. Journal of Composites for Construction (ASCE); 18(1), 04013026, http://dx.doi.org/10.1061/(ASCE)CC.1943-5614.0000384.

Laudiero F, Minghini F, Tullini N., 2013. Postbuckling failure analysis of pultruded FRP beams under uniform bending. Composites Part B: Engineering; 54: 431-438.

Minghini F, Tullini N, Laudiero F., 2009. Elastic buckling analysis of pultruded FRP portal frames having semi-rigid connections. Engineering Structures; 31(2): 292-299.

Minghini F, Tullini N, Laudiero F., 2010. Vibration analysis of pultruded FRP frames with semi-rigid connections. Engineering Structures; 32(10): 3344-3354.

Mosallam AD, Abdelhamid MK and Conway JH, 1994. Performance of pultruded FRP connections under static and dynamic loads. J. Reinf. Plast. Comp.; 13(5): 386-407.

Mottram J.T., 1999. Further tests on Beam to Column Connections for Pultruded Frames: Web – Cleated. Journal of Composites for Construction;3(1)

Mottram, J. T., 2011. "Does Performance Based Design with Fibre Reinforced Polymer Components and Structures Provide any new Benefits and Challenges?", *The Structural Engineer*, 89(6), 23-27.

Pecce, M. and Cosenza, E., 2000. "Local Buckling Curves for the Design of FRP Profiles", *Thin-Walled Structures*, 37(3), 207-222.

Russo S., 2013. 'Damage assessment of GFRP pultruded structural elements", Composite Structures, 96,pp. 661-669

Russo S., 2014. Investigation on buckling of all-FRP bolted built-up columns. The IES Journal Part A: Civil & Structural Engineering 2014;0(0):1-21, http://dx.doi.org/10.1080/19373260.2014.922450, Taylor and Francis.

Russo S., 2015. *Shear and local effect in all FRP bolted built-up columns*, Advances in Structural Engineering Journal, Vol.18, No.8

Russo, S., 2012. "Experimental and Finite Element Analysis of a Very Large Pultruded FRP Structure Subjected to Free Vibration", *Composite Structures*, 94(3), 1097-1105.

Russo, S., Boscato, G. and Mottram, J. T., 2012. "Design and Free Vibrations of a Large Temporary Roof FRP structure for the Santa Maria Paganica Church in L'Aquila, Italy". Presented at *6th International Conference on FRP Composites in Civil Engineering (CICE 2012)*, Section 8: All-FRP and Smart FRP Structures, Paper 209, 13th-15th June.

Shneider SP., 1998. Axially Loaded Concrete-Filled Steel tubes, Journal of Structural Engineering.

Smith SJ, Parsons ID, and Hjelmstad KD., 1999. Experimental comparisons of connections for GFRP pultruded frames. J. Compos. Constr.; 3(1): 20-26.

Steel Construction Manual, 13th Edition, 2006. American Institute of Steel Construction, AISC.
Structural Design of Polymer Composites, 1996. Eurocomp Design code and Background document; J.L. Clarke, CRC Press

Timoshenko SP, Gere JM., 1961. Theory of Elastic Stability. Mc Graw Hill, Second Edition.
Top Glass. Technical data, 1963. Material properties Triglass TM profiles. Top Glass SPA. www.topglass.it

Turvey GJ and Cooper C., 2004. Review of tests on bolted joints between pultruded GRP profiles. Proceedings of the Institution of Civil Engineers Structures & Buildings; 157(3): 211-233.

Turvey G.J., 1997. Analysis of pultruded glass reinforced plastic beams with semi-rigid end connections. Compos. Struct.; 38(1-4): 3-16.

Turvey, G. J., and Zhang, Y., 2006a. "A computational and experimental analysis of the buckling, post buckling and initial failure of pultruded GRP columns." Comput. Struct., 84(22-23), 1527-1537,

Turvey GJ, Zhang Y., 2006. Characterisation of the rotational stiffness and strength of web-flange junctions of pultruded GRP WF-sections via web bending tests. Composites Part A, 37(2), 152-164.

Turvey GJ, Zhang Y., 2006. Shear failure strength of web-flange junctions in pultruded GRP WF profiles. International Journal of Construction and Building Materials, 20(1-2), 81-89.

Vanevenhoven, L. M., Shield, C. K., and Bank, L. C., 2010. "LRFD factors for pultruded wide-flange columns." J. Struct. Eng. ASCE, 136(5), 554-564.

Mechanical properties	**Symbol**	**Value**
Longitudinal tensile strength	σ_z	350 MPa
Transversal tensile strength	$\sigma_x = \sigma_y$	70 MPa
Longitudinal elastic modulus	$E_z = E_l$	23 GPa
Transversal elastic modulus	$E_x = E_y = E_t$	8.5 GPa
Shear modulus	$G_{xy} = G_t$	3.4 GPa
Shear modulus	$G_{zx} = G_{zy} = G_{lt}$	3 GPa
Poisson's ratio	$\nu_{zx} = \nu_{zy} = \nu_{lt}$	0.23
Poisson's ratio	$\nu_{xy} = \nu_t$	0.09
Density	γ	1750 kg/mc
Fibres percentages (only glass)	V_f	40%
Fibres percentages (glass + carbon)	V_{hf}	40% - 5% (del 40%)

Table 1. Mean values of the mechanical characteristics of the FRP material [26].

"I" shape	λ	h, mm	$P_{cr(exp)\,kN}$
1-I12	9	120	732.0
2-I12	9	120	708.0
3-I12	9	120	706.0
1-I36	28	360	458.0
2-I36	28	360	438.0
3-I36	28	360	463.0
1-I60	46	600	240.0
2-I60	46	600	235.0
3-I60	46	600	227.1
3-I60	46	600	227.1
1-I100	78	1000	70.7
2-I100	78	1000	71.2
3-I100	78	1000	69.0
1-I150	117	1500	37.2
2-I150	117	1500	38.1
3-I150	117	1500	39.3
1-I200	156	2000	22.1
2-I200	156	2000	21.8
3-I200	156	2000	19.9
1-I250	196	2500	11.8
2-I250	196	2500	11.3
3-I250	196	2500	10.9

Table 2.Experimental critical loads and slenderness values for 'I' shape

"H"shape	λ	h, mm	$P_{cr(exp)}$ kN
1-H100	22	1000	720.8
2-H100	22	1000	692.3
3-H100	22	1000	695.5
1-H150	33	1500	708.1
2-H150	33	1500	661.3
3-H150	33	1500	688.8
1-H200	45	2000	620.8
2-H200	45	2000	651.9
3-H200	45	2000	635.0
1-H250	56	2500	552.8
2-H250	56	2500	542.7
3-H250	56	2500	524.3
1-H280	63	2800	606.7
2-H280	63	2800	477.8
3-H280	63	2800	492.0

Table 3. Experimental critical loads and slenderness values for 'H' shape

Specimen type	Cross-section dimension (d) and height (h)	λ	Thickness (t) - (mm)	d/t – b/t	P_{max} (kN)	Type of collapse
C1 circular	ϕ 120 mm h 120 mm	1.47	5	24 - /	603.3	Instability of hollow profile
C2 circular	ϕ 120 mm h. 1200 mm	14.74	5	24 - /	428.4	
C3 circular	ϕ 120 mm h. 2400 mm	29.49	5	24 - /	526.76	
Q1 square	(100x100) mm h 100 mm	1.35	10	/ - 10	1349.0	Instability of hollow profile with vertical break in the corner
Q2 square	(100x100) mm h 1200 mm	16.26	10	/ - 10	1244.6	
Q3 square	(100x100) mm h 1800 mm	24.39	10	/ - 10	850.11	
Q4 square	(100x100) mm h 2400 mm	32.52	10	/ - 10	795.8	
C152 channel	43x152 mm	22.6	9.5	/	11.1	*Flexural and torsional with evidence and without local damage*
C200 channel	60x200 mm	13.8	10	/	17.7	*Flexural and torsional even if in negligible way and Without local damage*

Table 4**.** Experimental results for only the FRP sample

Specimen type	Cross-section dimension (d) and height (h)- mm	λ	Thickness (t) (mm)	E-MPa	P_{max} (kN)	Type of failure
GN1Q Square	d=99 x99 h = 160	2.61	10	16887	1120	Loss of stress bond + vertical break in the corner
GN2Q Square	d=99 x 99 h = 160	2.61	10	/	550	Crush of concrete + vertical break in the corner
GN3Q Square	d=99 x 99 h = 160	2.61	10	/	569	Crush of concrete + vertical break in the corner
GN4Q Square	d=99 x 99 h = 106	1.73	10	/	569	Crush of concrete + vertical break in the corner
GN1C Circular	ϕ110 h = 220	3.89	5	23751	814	Loss of stress bond + instability of hollow profile
GN2C Circular	ϕ119 h = 220	3.61	5	/	592	Crush of concrete + crush of concrete; vertical break of FRP no local instability
GN3C circulae	ϕ120 h = 115	1.87	5	49327	680	Crush of concrete + crush of concrete; vertical break of FRP no local instability

Table 5. FRP/concrete square and circular samples, short columns

Specimen type	Dim.(mm)	$P_{max-exp}$(kN)	$P_{cr(e)}$ (kN)	P_{cr2} (kN)
GN1C circular	ϕ110; h 220	814.0	/	456.35
GN2C circular	ϕ 19 h 220	591.8	/	550.03
GN3C circular	ϕ 120 h 115	680.1	/	670.06
GN4C circular	ϕ 120 h 1200	679.1	932.3	329.78
GN1Q square	(99x99) h 160	1120.0	/	765.65
GN2Q square	(99x99) h 160	550.1	/	765.65
GN3Q square	(99x99) h 160	569.2	/	765.65
GN4Q square	(99x99) h 106	569	/	906.33
GN5Q square	(100x100);h 1200	824.4	826	237.81

Table. 6. Complex columns FRP/Concrete; experimental and predicted results

Formulation	P_{cr} *column 152 [kN]*	P_{cr} *column 200 [kN]*
Eq. (1)	335	1086
Eq. (2)	318	996
Eq. (21)	74	313
Eq. (2), λ from Eq. (23)	108	454
Eq. (2), λ from Eq. (24)	295	897
Eq. (2), λ from Eq. (25)	132	529
Experimental (mean value)	197	679
Calculation Method of l_r	l_r *(cm) Result of calculation*	l_{loc} *(cm)/* l_{tot} *(cm)length between connections/ height of column*
Form. (22), 3 bolted connection	376,26	91,3 / 273
Form. (22), 1 bolted connection, mid height	421,60	136,7 / 273
Form.(21) with P_{cr} exp, col.152	352	91,3 / 273
Form.(21) with P_{cr} exp, col.200	548,53	68,25 / 273

Table 7. Critical load values and calculated vale of reduced length l_r

Column configuration	Column characteristics	Eigenvalue FEA [kN]	Nonlinear FEA [kN]	Experimental [kN]
BC1	Column 152	230	213	148 (Test 1) 249 (Test 2) 193 (Test 3)
	Column 200	764	741	679
BC2	Column 152	238	270	365
	Column 200	945	904	1185
Type of profile	H (mm)	Cross section (mm)	P_{exp} (kN)	P_{cr} (kN) Formulation (33)
Hybrid	120	120x60x8	526,62	615
Hybrid	360	120x60x8	369,86	436
Hyibrid	600	120x60x8	113,83	182

Table 8. FEA and experimental buckling loads; . P_{cr} values for hybrid profiles

Figure 1. Built-up columns in an all FRP spatial truss structure and concrete foundation, [24], [25]

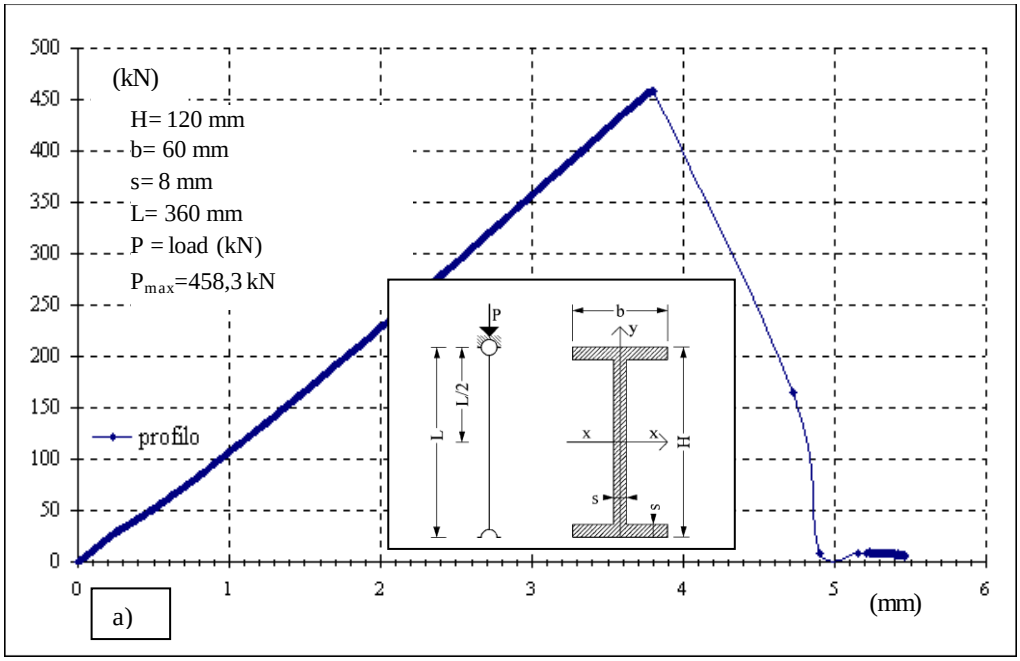

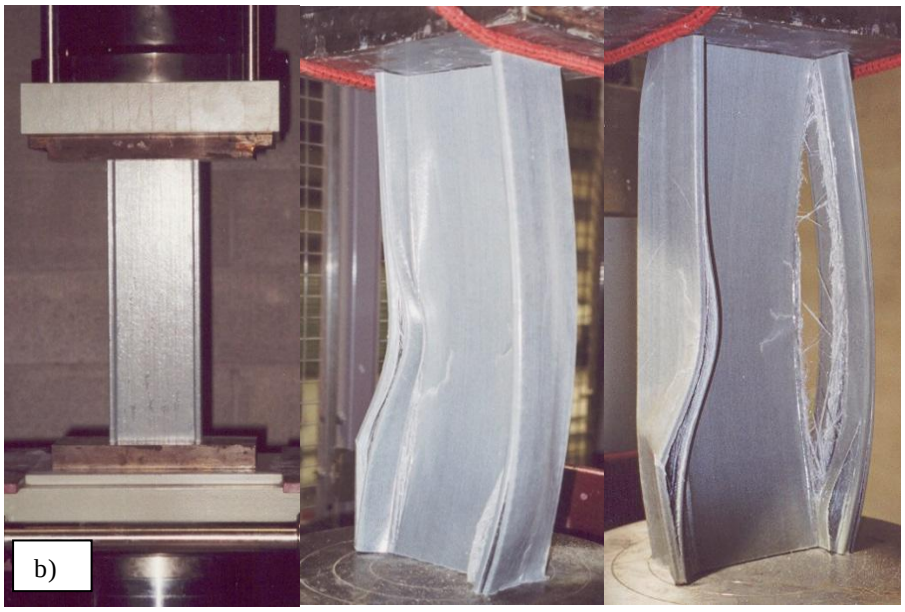

Figure 2. a) Load-axial displacement curve; b) failure mode. FRP column,"I" shape, h= 360 mm

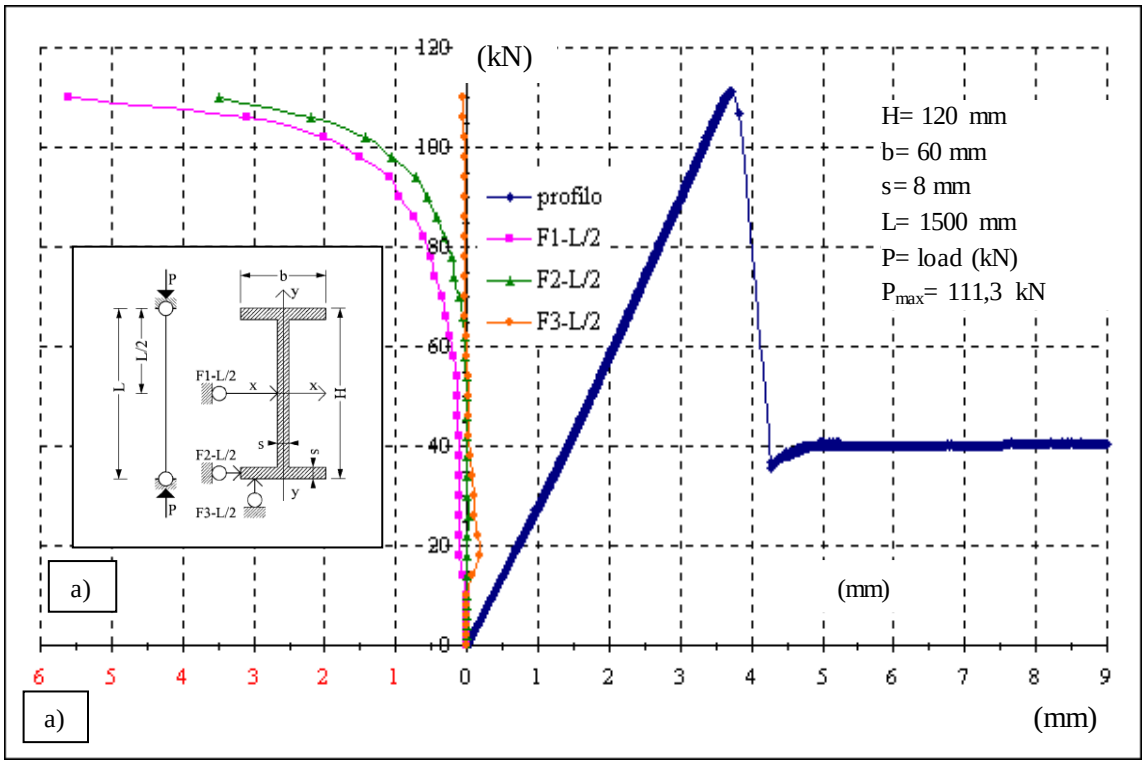

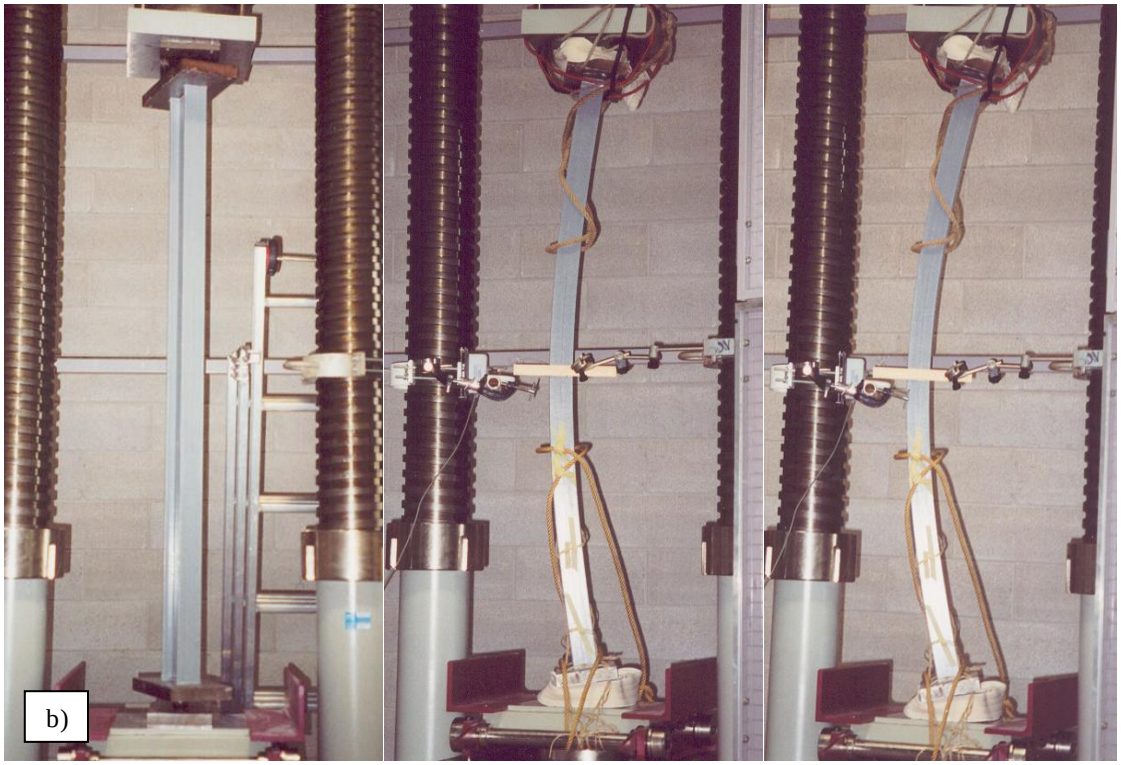

Figure 3. a)Load-axial displacement curve also with lateral displacement curves (coloured and on the left) at the half of the column; b) failure mode. FRP column,"I" shape; h=1500 mm

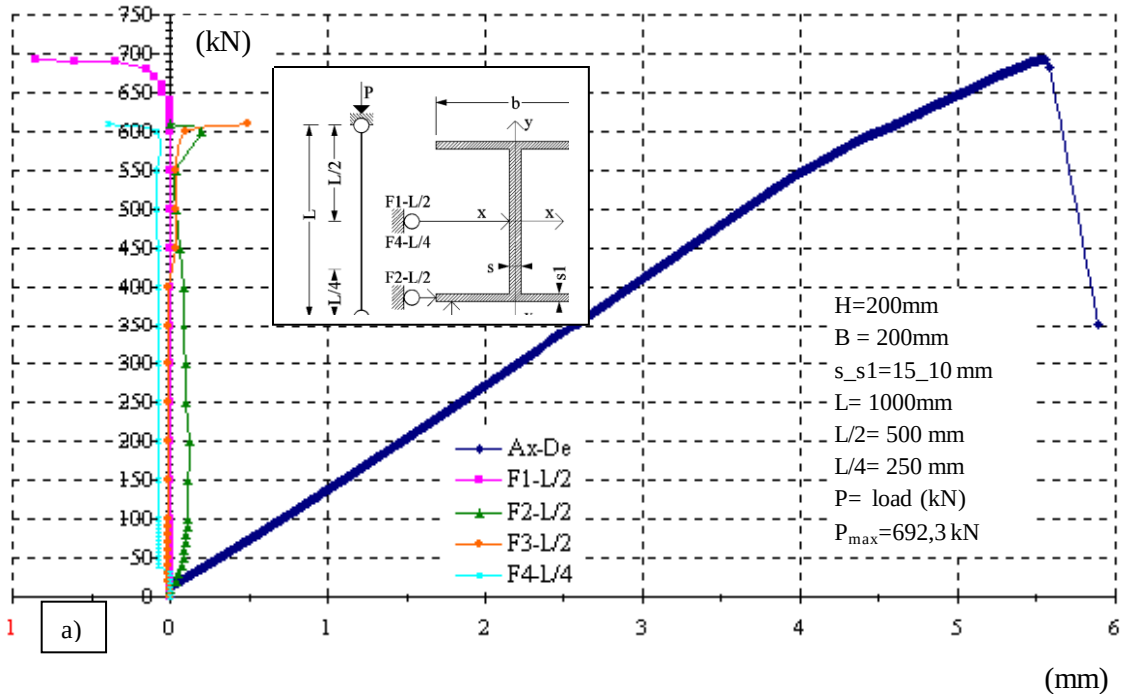

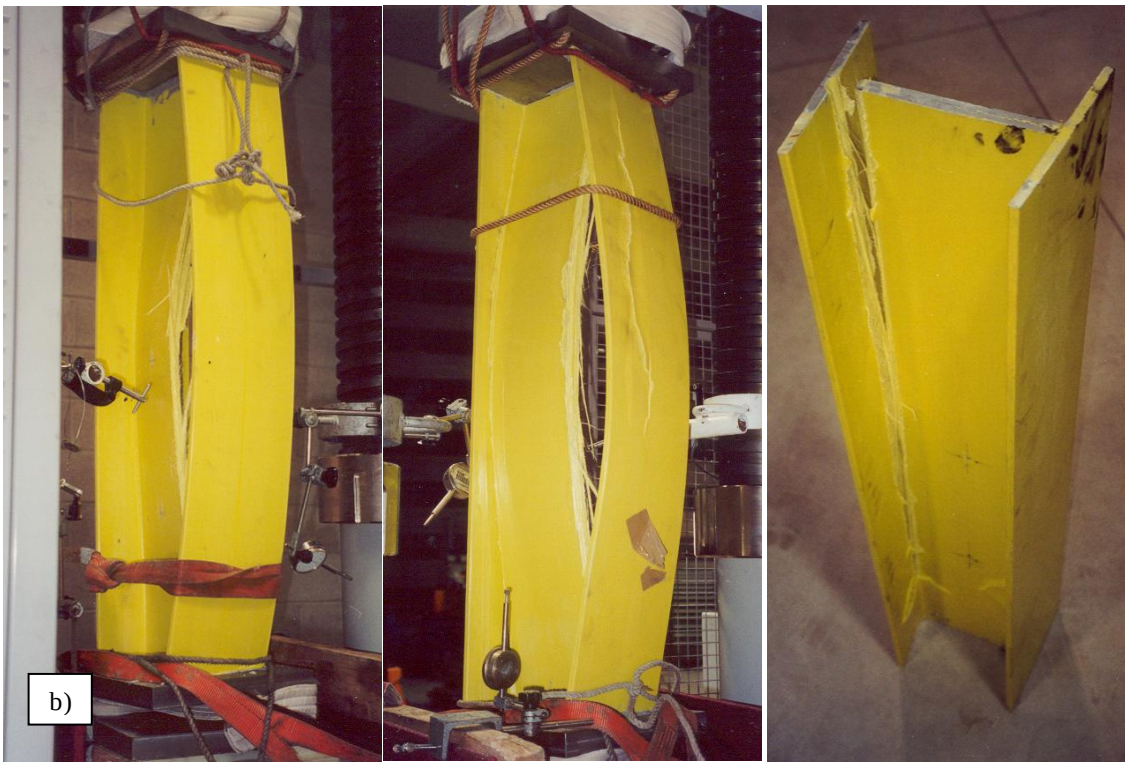

Figure 4. a)Load-axial displacement curve also with lateral displacement curves (coloured and on the left) at the half of the column; b) failure mode. FRP column,"H" shape; h=1000 mm

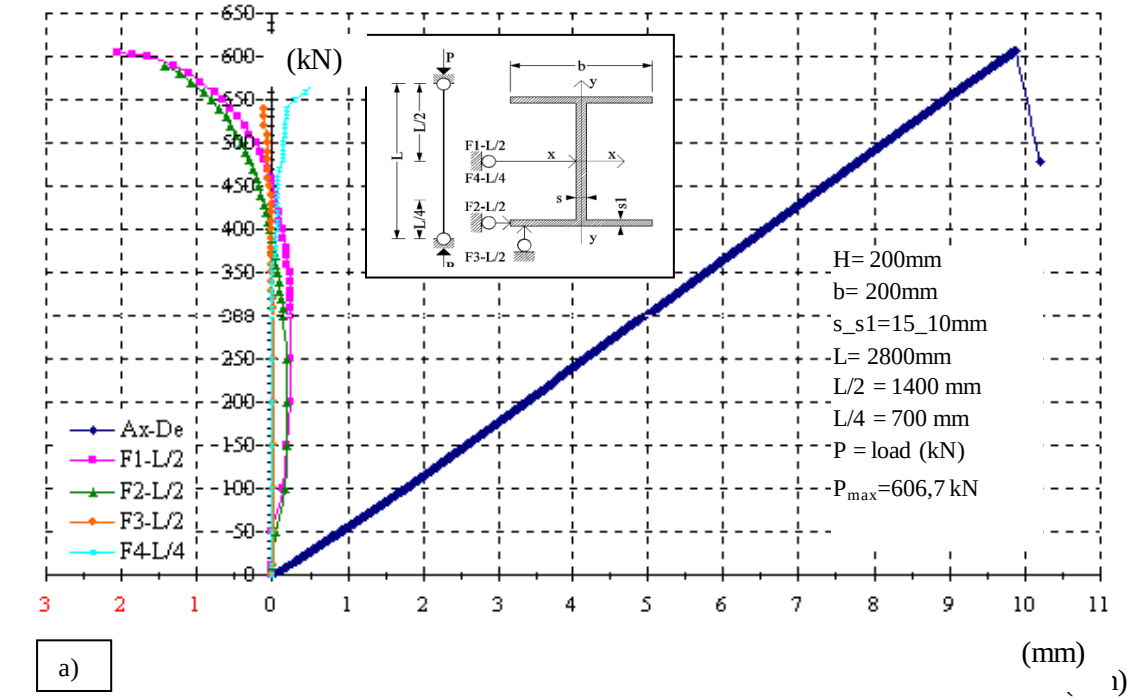

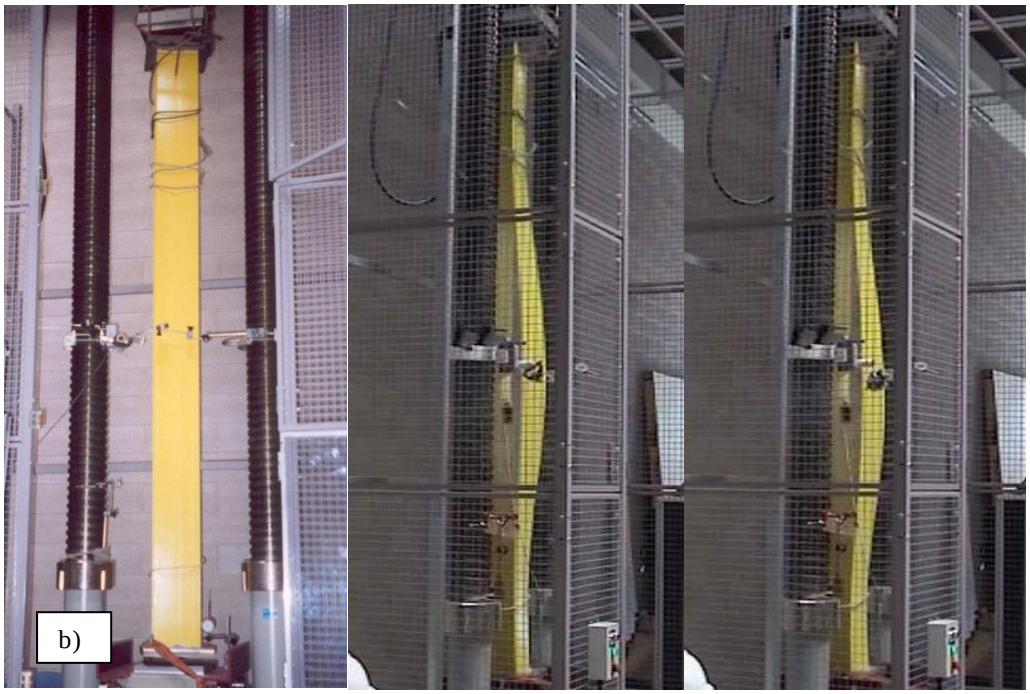

Figure 5. a)Load-axial displacement curve also with lateral displacement curves (coloured and on the left) at the half of the column; b) failure mode. FRP column,"H" shape; h=2800 mm

Figure 6. Typical collapses of complex column FRP/Concrete with very low values of λ

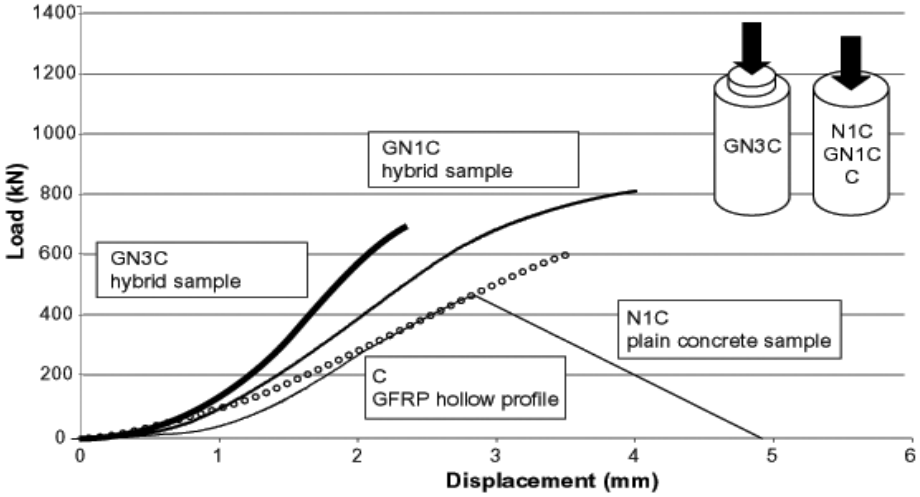

Figure 7. Load displacements curves for short circular samples with and without concrete

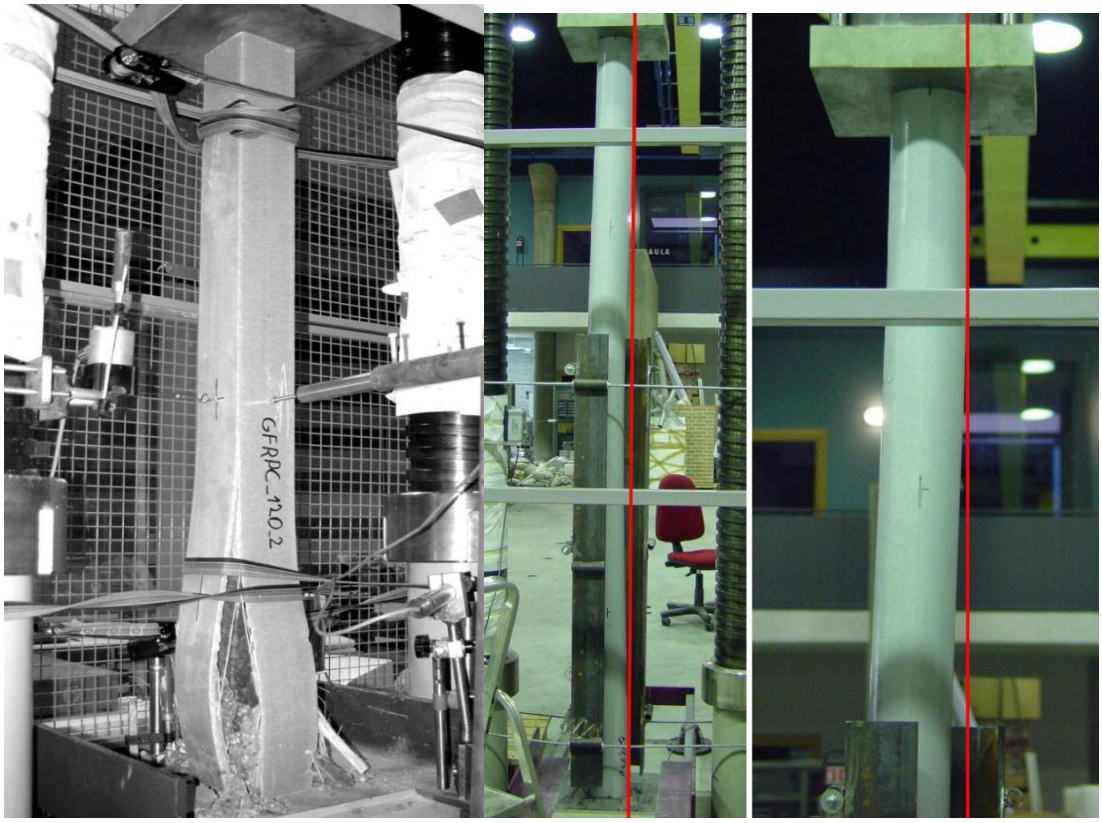

Figure 8.Collapse of FRP/Concrete columns with square and circular cross section; high values of λ

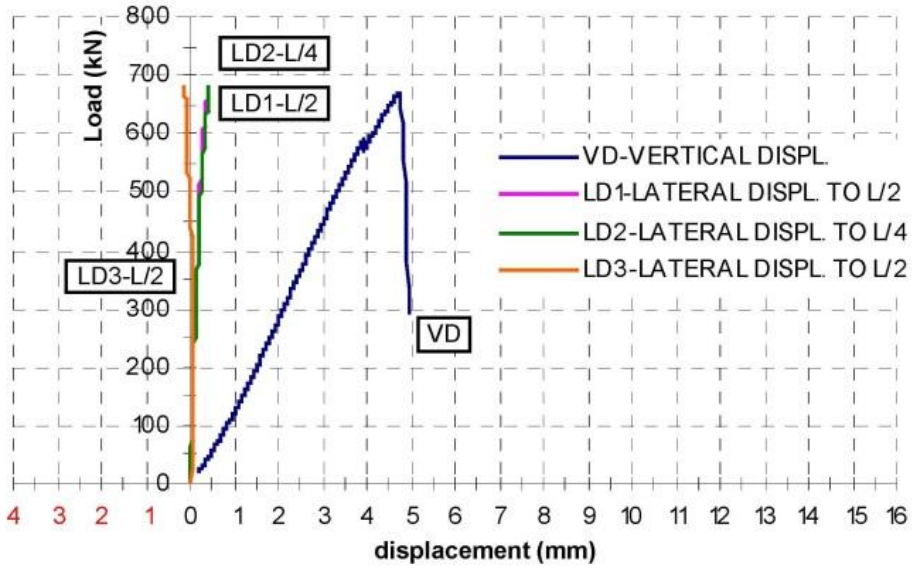

Figure 9. Load-displacement curves, FRP/Concrete, sample $\lambda = 19.51$

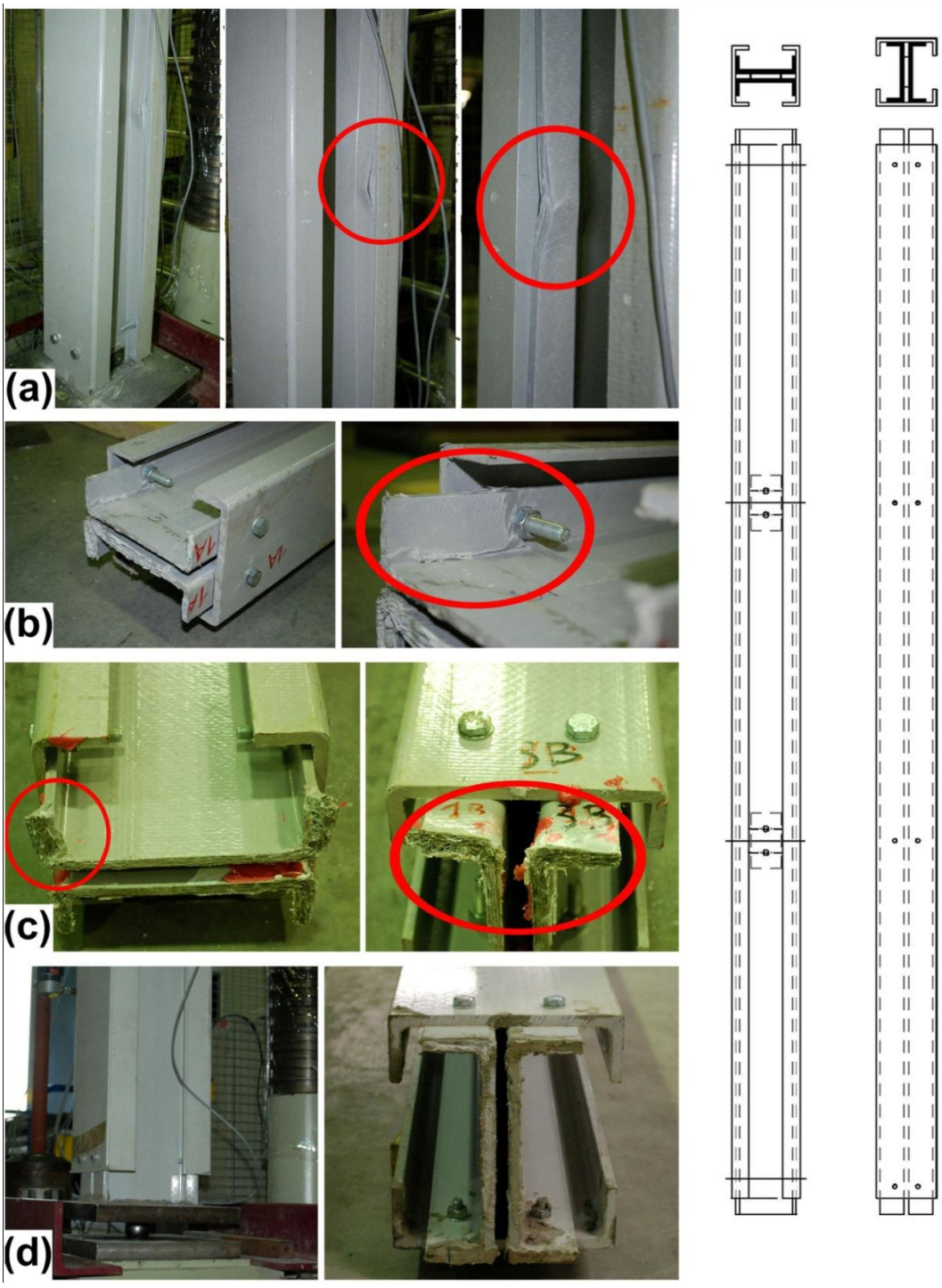

Figure 10. Loca/ global failure modes for built-up columns; load appli